



9-13-2022

Pulse-Echo Quantitative US Biomarkers for Liver Steatosis: Toward Technical Standardization

Timothy Stiles

David T. Fetzer

Ivan M. Rosado-Mendez

Michael Wang

Michelle L. Robbin

See next page for additional authors

Follow this and additional works at: https://digitalcommons.kettering.edu/naturalsci_facultypubs



Part of the [Physics Commons](#)

Authors

Timothy Stiles, David T. Fetzer, Ivan M. Rosado-Mendez, Michael Wang, Michelle L. Robbin, Arinc Ozturk, Keith A. Wear, Juvenal Ormachea, J. Brian Fowlkes, Timothy J. Hall, and Anthony E. Samir

Pulse-Echo Quantitative US Biomarkers for Liver Steatosis: Toward Technical Standardization

David T. Fetzer, MD* • Ivan M. Rosado-Mendez, PhD* • Michael Wang, PhD • Michelle L. Robbin, MD, MS • Arinc Ozturk, MD • Keith A. Wear, PhD • Juvenal Ormachea, PhD • Timothy A. Stiles, PhD • J. Brian Fowlkes, PhD • Timothy J. Hall, PhD • Anthony E. Samir, MD, MPH

From the Department of Radiology, University of Texas Southwestern Medical Center, Dallas, Tex (D.T.F.); Departments of Medical Physics (I.M.R.M., T.J.H.) and Radiology (I.M.R.M.), University of Wisconsin, Institutes for Medical Research, 1111 Highland Ave, Room 1005, Madison, WI 53705; General Electric Healthcare, Milwaukee, Wis (M.W.); Department of Radiology, University of Alabama at Birmingham, Birmingham, Ala (M.L.R.); Department of Radiology, Massachusetts General Hospital, Boston, Mass (A.O.); U.S. Food and Drug Administration, Silver Spring, Md (K.A.W.); Department of Electrical and Computer Engineering, University of Rochester, Rochester, NY (J.O.); Department of Natural Sciences, Kettering University, Flint, Mich (T.A.S.); Departments of Biomedical Engineering and Radiology, University of Michigan, Ann Arbor, Mich (J.B.F.); RSNA Quantitative Imaging Biomarkers Alliance (T.J.H.); and Center for Ultrasound Research & Translation, Department of Radiology, Massachusetts General Hospital, Harvard Medical School, Boston, Mass (A.E.S.). Received November 16, 2021; revision requested January 3, 2022; revision received April 7; accepted April 14. **Address correspondence** to I.M.R.M. (email: rosadomendez@wisc.edu).

Some images used in this article were acquired at Massachusetts General Hospital (MGH) for the Non-Invasive Biomarkers of Metabolic Liver Disease (NIMBLE) study (ClinicalTrials.gov identifier: NCT04828551, MGH IRB number: 2019P002092), supported by the Foundation for the National Institutes of Health (NIH). NIMBLE is a public-private partnership supported by AbbVie, Amgen, AstraZeneca, Boehringer Ingelheim, Bristol Myers Squibb, Echosens, GE Healthcare, Genentech, Gilead Sciences, Intercept Pharmaceuticals, Novo Nordisk A/S, Pfizer, Regeneron Pharmaceuticals, and Takeda Development Center Americas. NIMBLE also receives support from the Global Liver Institute and U.S. Food and Drug Administration. I.M.R.M. Supported by the Centennial Scholar Program, Office of the Vice Chancellor for Research and Graduate Education, Carbone Cancer Center, and Departments of Medical Physics and Radiology of the University of Wisconsin-Madison. A.E.S. Supported by the NIH National Institute of Diabetes and Digestive and Kidney Diseases (R01DK119860). Any opinions, findings, conclusions, or recommendations expressed in this material are those of the authors and do not necessarily reflect the views of the NIH.

* D.T.F. and I.M.R.M. contributed equally to this work.

Conflicts of interest are listed at the end of this article.

Radiology 2022; 305:265–276 • <https://doi.org/10.1148/radiol.212808> • Content codes:  

Excessive liver fat (steatosis) is now the most common cause of chronic liver disease worldwide and is an independent risk factor for cirrhosis and associated complications. Accurate and clinically useful diagnosis, risk stratification, prognostication, and therapy monitoring require accurate and reliable biomarker measurement at acceptable cost. This article describes a joint effort by the American Institute of Ultrasound in Medicine (AIUM) and the RSNA Quantitative Imaging Biomarkers Alliance (QIBA) to develop standards for clinical and technical validation of quantitative biomarkers for liver steatosis. The AIUM Liver Fat Quantification Task Force provides clinical guidance, while the RSNA QIBA Pulse-Echo Quantitative Ultrasound Biomarker Committee develops methods to measure biomarkers and reduce biomarker variability. In this article, the authors present the clinical need for quantitative imaging biomarkers of liver steatosis, review the current state of various imaging modalities, and describe the technical state of the art for three key liver steatosis pulse-echo quantitative US biomarkers: attenuation coefficient, backscatter coefficient, and speed of sound. Lastly, a perspective on current challenges and recommendations for clinical translation for each biomarker is offered.

© RSNA, 2022

The abnormal accumulation of liver fat, known as steatosis, has significant clinical implications. The most common form is nonalcoholic fatty liver disease (NAFLD) (1). Given the association with obesity, type 2 diabetes, hyperlipidemia, and hypertension, a new term has been proposed: metabolic dysfunction–associated fatty liver disease, or MAFLD (2). NAFLD affects nearly one-quarter of the general population and up to two-thirds of individuals with type 2 diabetes mellitus (2,3). Other causes of liver steatosis include excessive alcohol intake, viral hepatitis, metabolic storage disorders, and drugs and toxins (4).

NAFLD encompasses a wide range of disease states, including isolated steatosis and nonalcoholic steatohepatitis; the latter is defined by the presence of steatosis, lobular inflammation, hepatocyte ballooning, and perisinusoidal fibrosis deposition (5). Nonalcoholic steatohepatitis affects 1.5%–6.5% of the worldwide population and may progress to advanced fibrosis (incidence 67.95 in 1000 person-years), with associated liver-specific mortality (11.77 per 1000 person-years) and hepatocellular carcinoma (5.29 per 1000 person-years) (1). NAFLD is now the most common cause of chronic liver disease

worldwide, affecting nearly 1 billion individuals, and is an increasingly common indication for liver transplant in the United States (6,7). NAFLD is also an independent risk factor for cardiovascular disease, which remains the most common cause of death in this population (3,8).

Although hepatic steatosis is a common finding with multiple modalities, including US, CT, and MRI, radiologists must remain vigilant regarding its presence and severity. The simple presence of steatosis can be a sign of systemic metabolic derangements (metabolic syndrome) for which other imaging markers exist, including increased visceral fat, fatty pancreatic replacement, and epicardial and pericardial fat (9). The degree of liver fat during the initial diagnostic study is also important. At least one longitudinal study (10) has shown significantly higher odds of fibrosis progression in patients with higher liver fat content at baseline. Several clinical trials have adopted changes in liver fat as an end point to assess the efficacy of interventional treatments (11,12). According to one study, a 30% reduction in liver fat, estimated with the MRI proton density fat fraction (PDFF), was associated with a two-point improvement

Abbreviations

AC = attenuation coefficient, AIUM = American Institute of Ultrasound in Medicine, BC = backscatter coefficient, NALFD = nonalcoholic fatty liver disease, PDFF = proton density fat fraction, PEQUS = pulse-echo quantitative US, QIBA = Quantitative Imaging Biomarkers Alliance, SOS = speed of sound

Summary

Standardization of technical performance and clinical implementation of pulse-echo quantitative US is essential for the development of fit-for-purpose sonographic liver steatosis biomarkers.

Essentials

- There is an urgent need for practical, objective, and noninvasive means for diagnosing, stratifying, and monitoring liver steatosis.
- This need has prompted efforts to implement pulse-echo quantitative US (PEQUS) technology in commercial US scanners.
- PEQUS is based on quantifying acoustic properties of tissue, including the attenuation coefficient, backscatter coefficient, and speed of sound, in a system-independent manner.
- Continuous development over the past 40 years has produced evidence of the potential value of PEQUS properties as liver steatosis biomarkers.
- To facilitate the translation of these biomarkers into clinical practice, health care professionals, scientists, and industry and government representatives are working together in a public-private partnership facilitated by the RSNA Quantitative Imaging Biomarkers Alliance.

in the NAFLD activity score as assessed by liver histologic findings (13). Increasing NAFLD incidence combined with the emergence of liver fat-reducing therapies has created an important unmet need for a widely available and cost-effective liver fat quantification test that will permit at-risk patient screening and risk stratification, and that can be safely applied serially for disease monitoring.

Biomarkers of Liver Steatosis

Biopsy has traditionally been considered the standard of care for liver disease assessment. Histologically, liver fat content is subjectively graded by the number of involved hepatocytes, from S0 (no steatosis) to S3 (severe steatosis). Scoring algorithms for NAFLD, such as the Nonalcoholic Steatohepatitis Clinical Research Network system, the fatty liver inhibition of progression (FLIP) score, and the NAFLD activity score, rely on the steatosis grade as well as the inflammation activity and fibrosis stage (14–16). However, histologic assessment is known to be limited by sampling error and interobserver variability (17,18). Moreover, biopsy is relatively expensive and invasive, with a slight, although definite, risk of serious complications; thus, it is impractical for disease screening and monitoring, particularly given the high prevalence of NAFLD and nonalcoholic steatohepatitis (19–21). Accurate, cost-effective, and noninvasive steatosis biomarkers are needed.

According to the Biomarkers, EndpointS, and other Tools (BEST) glossary developed jointly by the U.S. Food and Drug Administration and National Institutes of Health, a biomarker is a “characteristic that is measured as an indicator of a normal biological process or a pathogenic process, or the biological response to an exposure or intervention, including therapeutic



Figure 1: Image shows the controlled attenuation parameter (CAP), which is a nonimaging sonographic method to estimate steatosis available on a vibration-controlled transient elastography point-of-care device (FibroScan; Echosens).

interventions” (22). Biomarkers can be used for risk stratification, diagnosis, surveillance, prognosis, or safety monitoring.

Many biomarkers are currently in clinical use for the management of chronic liver disease, with varying sensitivity and specificity for steatosis. Combinations of patient characteristics and individual serum values may be used in scoring systems such as the fatty liver index, hepatic steatosis index, SteatoTest (BioPredictive), and nonalcoholic fatty liver screening score, which predict NAFLD with an area under the receiver operating characteristic curve of 0.84, 0.82, 0.80, and 0.83–0.86, respectively (23,24). However, these panels perform poorly in mild steatosis and may not be sensitive enough to detect changes on a scale needed for disease monitoring.

The controlled attenuation parameter (Fig 1), a nonimaging sonographic method of estimating steatosis, is available on a vibration-controlled transient elastography point-of-care device (FibroScan; Echosens). In a recent meta-analysis (25), areas under the receiver operating characteristic curve to detect patients with a histopathologic steatosis stage of S0 versus S1–3 and S0–1 versus S2–3 were 0.81 (95% CI: 0.76, 0.86) and 0.75 (95% CI: 0.72, 0.78), respectively. Liver stiffness, measured with the same device, was recently combined with the controlled attenuation parameter and serum levels of aspartate transaminase and alanine transaminase in a logistic regression model called FibroScan-AST (or FAST). Variable positive predictive values were found in an external validation cohort, with a negative predictive value of 73%–100% (26). Cutoffs vary in the literature, with

variations in negative and positive predictive values reported, and with overlap across different steatosis grades (27). In patients with obesity, NALFD steatosis grading can be limited by body wall thickness (25,28,29).

Imaging devices may also provide liver steatosis measurements. CT measurements of x-ray attenuation, in Hounsfield units, can estimate liver fat by the decrease in absorption. Although CT has high sensitivity (72%–95%) and specificity (90%–99%) for the detection of moderate steatosis, it does not perform as well in mild steatosis (30–32). Noncontrast CT is more accurate than contrast-enhanced CT, as iodinated contrast material increases normal liver attenuation (31,32). Dual-energy CT is more accurate than single-energy CT in liver fat quantification, particularly for examinations performed with intravenous contrast material (33–35). Unfortunately, CT attenuation is also affected by edema, iron, copper, glycogen, and amiodarone (36). CT may play a role in opportunistic screening when performed for other purposes (37); however, because ionizing radiation is required, other modalities, such as MRI and US, may be preferred for surveillance.

Various MRI techniques are available for detecting and quantifying liver fat, which are well summarized in a recent review by Starekova et al (32), leveraging the differences in precession frequency between water and lipid-associated hydrogen. MR spectroscopy is arguably the most accurate method, relying on the measurement of the lipid peak on a ^1H MR spectrum, although it is limited to a small sampling region of interest and is only available at centers with specific expertise (31,32). Dual-echo chemical shift imaging is widely available and reproducible, allowing for the qualitative detection of intracellular lipid by loss of signal when opposing magnetizations of water and fat within the same voxel are summed (31). The MRI-derived proton density fat fraction (PDFF) has emerged as an accurate and precise quantitative technique (38,39) for measuring the confounder-corrected proportion of lipid-associated hydrogen signal within a specified volume, and correlates well with histologic grade ($r = 0.743$) (40). PDFF thresholds of 5%, 15%, and 25% have been proposed for mild, moderate, and severe steatosis, respectively (32). Benefits of the MRI PDFF include whole-liver assessment and the ability to perform elastography and iron quantification in the same setting (20,32,41). Although the MRI PDFF may function as a robust confirmatory test, cost and lack of widespread availability may impact the practicality of population screening and longitudinal disease monitoring.

B-mode US has been used for decades as an inexpensive noninvasive method of hepatic fat evaluation. Liver fat increases acoustic absorption (conversion of acoustic energy to heat) and scattering (redirection of acoustic energy); both phenomena contribute to increased attenuation (31). In addition, increased acoustic energy reflected back to the transducer (ie, backscattered) is seen as increased echogenicity or brightness on an image. Although echogenicity increases with worsening steatosis, B-mode US brightness is also dependent on factors such as transmit power, focusing, and gain, as well as attenuation by interposed soft tissues such as subcutaneous fat. Therefore, the qualitative assessment of echogenicity requires a comparison with an internal reference such as the spleen or right kidney cortex, which itself

requires an absence of conditions that may alter echogenicity of these adjacent organs. Other visual features include loss of the echogenic portal walls and appearance of areas of focal fat sparing. Increased acoustic attenuation causes the far field to appear progressively darker without adjustments to the transmit pulse power, transmit frequency, and time-gain compensation. This, as well as the relative increase in parenchymal echogenicity, leads to reduced conspicuity of the diaphragm. Liver fat also decreases the speed of sound (SOS) in tissue, which leads to flawed beam focusing and degraded spatial resolution.

A meta-analysis of 34 studies, which included 2815 patients and liver biopsy as the reference (42), reported a pooled sensitivity and specificity of 85% and 93%, respectively, for US in distinguishing moderate-to-severe steatosis from normal. However, qualitative US is insensitive to mild steatosis (43) and subjective assessment is likely dependent on the manufacturer, transducer, frequency, waveform characteristics, and experience of the operator (44). The hepatorenal index was developed as a semiquantitative method to overcome some of these challenges by measuring the ratio of mean brightness of liver and adjacent renal cortex at the same depth (45,46). Chauhan et al (47) found that both subjective evaluation and the hepatorenal index reached 100% sensitivity, although the latter was more specific at 95.2%. The hepatorenal index assumes a normal renal cortex and, therefore, it may be inaccurate in various stages of acute or chronic kidney disease. The hepatorenal index is also of limited utility in differentiating between mild and no steatosis, and there is no consensus on cutoff values (47). For all these techniques, confounders include fibrosis, glycogen, and infiltrative processes, which may also increase liver echogenicity. True quantitative US biomarkers may offer a pathway to overcome these limitations of qualitative assessment.

Potential PEQUS Biomarkers for Liver Steatosis

The system and operator dependence of B-mode US has limited its efficacy as an objective clinical decision-support tool thus far. To overcome this limitation, quantitative features that describe attenuation, backscattering, and SOS can serve as pulse-echo quantitative US (PEQUS) imaging biomarkers. These features are the attenuation coefficient (AC), backscatter coefficient (BC), and SOS (48). The following sections expand on the technical principles for the quantification of these three parameters and provide a perspective on the history of their development and challenges to implementation.

Attenuation Coefficient

The AC describes the rate of amplitude decrease of the ultrasound waves as they travel through tissue. Ultrasound waves that travel in more attenuating tissue lose more amplitude (a loss quantified in decibels) over the same propagation distance (expressed in centimeters) than in less-attenuating tissues. On average, attenuation in the liver increases approximately proportionally with frequency. As a result, the AC is expressed in decibels per centimeter at a specified frequency (units of dB/cm-MHz). Several attenuation estimation methods have been proposed, including spectral shift, sound field correction, spectral difference, spectral log difference, and hybrid methods (49).

Studies in the 1980s showed a clear association between the AC and steatosis (50–53). However, limitations, such as system and operator dependence and measurement variability, and confounding factors, such as fibrosis, fasting state, glycogen accumulation, and breathing, were not well understood at that time. These concepts are now the subject of several clinical trials. Currently, AC measurement methods are commercially available with several clinical US imaging systems (54). Some implementations are based on point-wise measurements producing a single AC value from a region of interest, while other implementations produce parametric images of the AC, which show the spatial distribution of AC values in a color scale. In a recent meta-analysis that included implementations from several manufacturers, the pooled sensitivity and specificity of the AC feature were 76% (95% CI: 73, 80) and 84% (95% CI: 77, 89), respectively, to detect patients with a histopathologic steatosis stage greater than or equal to S1 and 87% (95% CI: 83, 91) and 79% (95% CI: 77, 89), respectively, to detect patients with a steatosis stage greater than or equal to S2 (55).

Understanding the overall bias, variability, and operator dependence of AC implementations requires large clinical trials. For example, the accuracy and variability of AC values in patients with thick subcutaneous fat might be affected by various artifacts, such as reverberations and clutter (56). Considering the correlation between high subcutaneous fat-tissue thickness and hepatic steatosis, understanding the impact of these artifacts will be necessary. Additionally, in patients with steatosis, superimposed hepatic inflammation and fibrosis may also confound estimates of technical and clinical performance (57). Because most vendors provide shear-wave elastography and attenuation technologies in the same US system, the former could be used to assess for co-occurrence of fibrosis. Prospective multivendor, multisite clinical trials may be needed to understand the magnitude of these limitations. Currently, vendors use different methods to measure the AC; therefore, merging all published results and performing a cumulative analysis is challenging for meta-analyses.

Backscatter Coefficient

Backscatter, the primary determinant of gray-scale brightness on B-mode images (ie, tissue echogenicity), occurs when the incident wave interacts with unresolvable submillimeter variations in density and compressibility that compose the tissue stroma. Backscatter may be quantified for a volume of tissue (such as liver) by the BC, an absolute metric of the acoustic power (W) redirected back to the transducer (scattered at 180°) within a small solid angle (steradian [Sr], which is a unit of solid angle and technically defined as the solid or three-dimensional angle subtended at the center of a sphere with a radius of 1 cm by an area of 1 cm^2 on its surface) over the incident intensity (W/cm^2), divided by the volume containing the scatterers (cm^3). Thus, the units for BC are one over centimeter per steradian ($W/Sr/[W/cm^2]/cm^3 = 1/cm-Sr$) (58).

The most common method for measuring BC in vivo with a clinical US system is the reference phantom method (59). This requires paired pulse-echo measurements in vivo and in a

reference phantom with known AC and BC reference values. US imaging system settings are kept constant between human and phantom measurements to correct for gain and region of interest location. In practice, the need to acquire data from a reference phantom can be eliminated by integrating previously acquired reference data in the scanner (60,61). This strategy would require ensuring consistency in scanner and transducer performance, thus making routine quality control even more important. For studies in human liver, the most common choice of US frequency is near 3 MHz (61–65) because higher frequencies can have inadequate penetration depth.

Early in vivo measurement of human liver BCs in small cohorts ($n = 13, 15, 35$) established a normal mean range of approximately $4 \times 10^{-4} 1/cm-Sr \pm 2$ (SD) for frequencies from 2.25 MHz to 3 MHz (61,62,66). In one of these early studies, liver fat in seven patients resulted in a mean BC of $68 \times 10^{-4} 1/cm-Sr \pm 37$ (66), an elevation of more than an order of magnitude. Recently, the BC has been tested in larger-scale clinical trials. In one study ($n = 204, 3\text{ MHz}$), the BC correlated with the MRI PDFF, with a Spearman rank correlation coefficient of 0.80 (64). In another study ($n = 102, 2.7\text{ MHz}$), patients with MRI PDFFs ranging from 0.7% to 41% (mean, 12.8%) exhibited an elevated mean BC of $45 \times 10^{-4} 1/cm-Sr \pm 55$ (65). In another study ($n = 101, 3\text{ MHz}$), a quadratic model of log-transformed BC ($dB/cm-Sr$) resulted in a coefficient of determination of $R^2 = 0.76$ for MRI PDFF estimates of liver steatosis (61). In summary, these studies suggest that the BC could potentially be used as a surrogate for the MRI PDFF.

Improving the clinical performance of US backscatter for assessing liver fat fraction will involve addressing several challenges. First, an accurate, consistent method must be developed to compensate backscatter measurements for the effects of attenuation from abdominal wall fat and muscle, and the liver itself (66,67). Second, an optimal method must be developed for positioning the transducer, which might include efforts such as avoiding blood vessels, portal tracts, and focal lesions (68); avoiding large bile ducts (69); and situating the ultrasound beam as close to perpendicular to the liver capsule as possible, likely using similar techniques as those for performing shear-wave elastography (69). Third, measurement variations due to operator dependence (70), fasting state (71), system parameters (eg, transducer geometry, center frequency, bandwidth, beamforming algorithm), and phase aberration caused by subcutaneous adipose tissue must be understood and minimized.

Speed of Sound

The SOS describes how fast ultrasound waves travel through a tissue, and its square value is inversely related to the density of tissue and its compressibility. Thus, ultrasound waves travel faster in less compressible tissues. The SOS should not be confused with the speed of shear waves used in shear-wave elastography to evaluate tissue stiffness. Shear-wave speed is related to the shear modulus, which quantifies the resistance of a material to change its shape, while the SOS is mainly defined by the bulk modulus (inverse compressibility) (72). The shear-wave speed has been proposed as a biomarker for liver fibrosis, which has been reviewed excellently by Barr (73). Conventionally, clinical

Summary of Pulse-Echo Quantification of Liver Fat Using Transabdominal US

Characteristic	Attenuation	Backscatter	Speed of Sound
Physics principle	Rate of acoustic power loss due to absorption and scatter; frequency dependent	Proportion of acoustic power reflected back to transducer; frequency dependent	Velocity of sound in specific tissue; relatively independent of frequency
Correlation with biologic concept (steatosis)	Observed to increase with increasing liver fat	Observed to increase with increasing liver fat	Observed to decrease with increasing liver fat
Biomarker; unit of measurement	Attenuation coefficient; decibels per centimeter per megahertz (dB/cm-MHz)	Backscatter coefficient; 1 over centimeter per steradian (1/cm-Sr) or decibels with respect to this unit	Speed of sound; meters per second (m/sec)
Approximate reference range, from healthy to advanced steatosis	0.5 to 1.3 dB/cm-MHz at 3 MHz (43,48,54,61)	10^{-4} to 10^{-2} 1/cm-Sr at 3 MHz (43,61,63,65,66)	1590 to 1470 m/sec (92)
Opportunities and benefits	Already available in scanners by several vendors	Provides objective assessment of liver echogenicity without the need of a reference tissue (eg, kidney)	Physically intuitive and easy to interpret
Challenges and limitations	Bias introduced by reverberations, clutter, and blood vessels; variability in quantification methods may complicate standardization; possible confounding effects of inflammation and fibrosis	Depends on accurate compensation for intervening tissue attenuation; the need for reference calibration may result in stricter system and transducer performance criteria; possible confounding effects of inflammation and fibrosis	Small percentage change between normal and disease states; limited number of methods that provide local speed of sound estimates; possible confounding effects of inflammation and fibrosis

US systems assume a fixed value for SOS during beamforming (1540 m/sec in most cases), as a key input when performing echolocation for image formation. The assumed SOS is typically held constant for the whole image. However, different tissues may have different SOS values, resulting in image quality degradation.

The three most promising strategies to quantify SOS are based on focusing (74,75), spatial coherence (76–78), and compounding methods (79–81). Focusing techniques estimate SOS by adjusting the assumed sound speed in beamforming to maximize image quality metrics, such as lateral resolution. Compounding methods estimate the SOS by applying varying transmit beam directions to measure the resultant local phase changes. Spatial coherence methods estimate the SOS by maximizing the coherence of echoes from a target region.

Several SOS values for in vivo human liver tissue (74,77,78,81–85) and liver specimens (82,86) have been reported in different studies. Overall, hepatic SOS varies from 1450 m/sec to 1650 m/sec, depending on the underlying pathologic abnormality. Normal liver has an SOS value of approximately 1560 m/sec, while steatotic and cirrhotic livers have shown a lower and higher SOS, respectively. For example, Chen et al (84) reported mean SOS values of 1547 m/sec \pm 17.8 for fatty livers and 1610 m/sec \pm 30 for cirrhotic livers. The mean values reported by Hayashi et al (74) were 1423 m/sec \pm 34 and 1558.3 m/sec \pm 23.2 for fatty and cirrhotic livers, respectively. On the other hand, Boozari et al (87) reported mean SOS values of 1575 m/sec \pm 21 and 1594 m/sec \pm 18 for hepatic fibrosis for stages F0–F3 and F4, respectively. More recently, Popa et al (88) determined a cutoff value of 1537 m/sec or lower for predicting the presence of liver steatosis. Studies have shown reliability between operators as well as accuracy

when compared with pathologic findings (89) or MRI PDFFF results (78,90). Likely confounders include liver fibrosis, inflammation, subcutaneous fat effects, and depth dependence, which are similar to those of the AC and BC (48,91,92).

While promising, additional studies are needed to standardize the measurement of hepatic SOS and to determine the expected measurement variability. This is particularly important for SOS due to the relatively small percentage change in disease states compared with normal. Thus, high precision measurement will be required. Further studies are also needed to confirm correlation with hepatic fat levels, to define specific thresholds, and to detect and mitigate covariates that may influence hepatic SOS.

Summary of PEQUUS Biomarkers

The three proposed PEQUUS biomarkers are summarized in the Table, where the physical principles underlying each biomarker (represented graphically in Fig 2), observed correlation with steatosis, unit of measurement, approximate reference range, and opportunities and challenges for implementation are described. Figures 3–6 show examples of commercial implementations of PEQUUS biomarkers. Currently, there are insufficient data and head-to-head comparisons to recommend one PEQUUS biomarker or implementation over another.

Standardization of Quantitative Imaging Biomarkers

Quantitative measurements derived from medical images yield quantitative imaging biomarkers, which are defined as “an objective characteristic derived from an in vivo image measured on a ratio or interval scale as an indicator of normal biological processes, pathogenic processes or a response to a therapeutic intervention” (93).

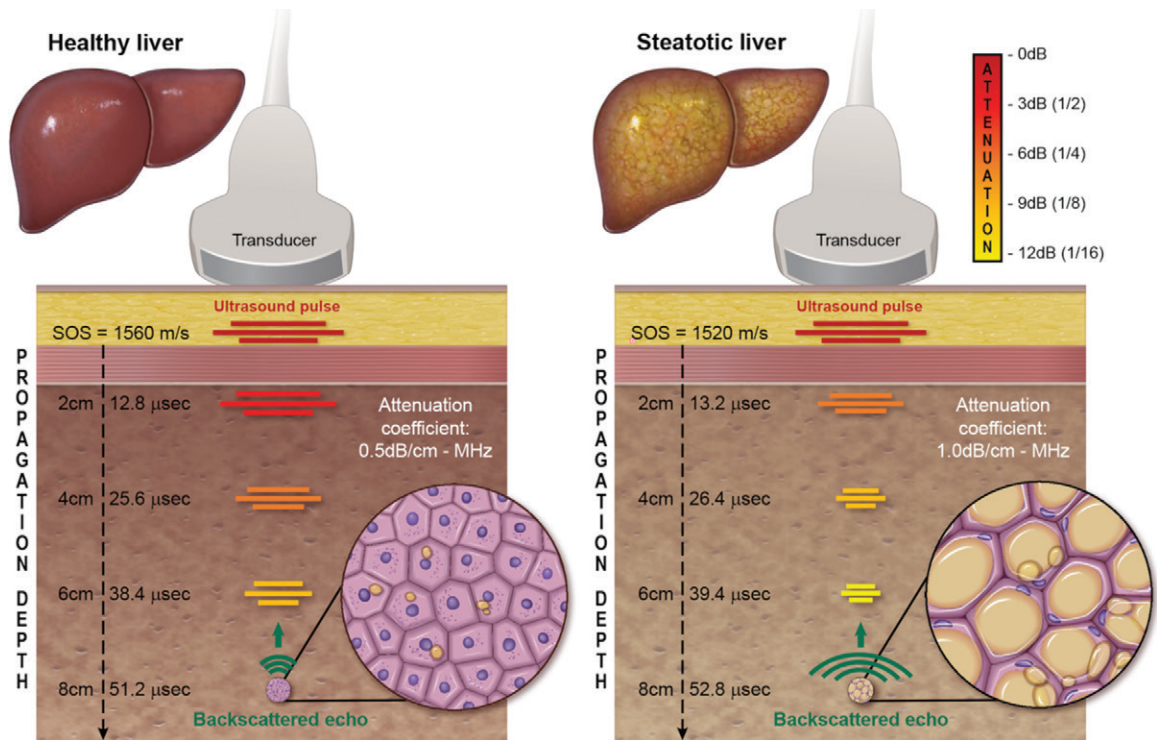


Figure 2: Diagrams depict the physics principles behind three PEQUS biomarkers—attenuation coefficient (AC), backscatter coefficient, and speed of sound (SOS)—for (left) healthy liver and (right) steatotic liver. The color bar legend at the top right indicates ultrasound pulse amplitude as it travels through tissue and is attenuated to a great extent in steatotic liver (AC of 1.0 dB/cm-MHz). The inserts show the liver microstructure that produces backscattered echo, which is greater in steatotic liver due to hepatocytes filled and expanded by lipid vacuoles. The vertical array of numbers on the left side of each diagram indicates the propagation depth and time of ultrasound pulse arrival based on the SOS reported at the top of the array.

Evaluation of technical and clinical performance is a central challenge in quantitative imaging biomarker development. Technical performance is defined as a measure of the level of confidence in the measuring process itself, whereas clinical performance is defined as the correlation between the biomarker and the biologic process of interest. These processes require rigorous development, followed by validation in the intended biomarker context of use. There are currently several organized efforts to develop standardized strategies to assess biomarker technical and clinical performance. The RSNA Quantitative Imaging Biomarkers Alliance (QIBA) was created in 2007 to address the need for standardization of technical performance, with a mission to “improve the value and practicality of quantitative imaging biomarkers by reducing variability across devices, patients, and time” (94). QIBA is divided into biomarker committees, with each committee working toward developing biomarker profiles. The profiles are guidelines for standardizing biomarker quantification to meet technical performance claims, including bias (difference between the expected value of the measured characteristic and its true value) and sources of variability, such as levels of repeatability (measurement error when measuring conditions do not vary [same sample, same measuring device, same operator]) and reproducibility (measurement error when conditions vary [different measuring device, different operator]) (95). In addition to the performance claims, the profile defines a series of activities that different actors, such as the manufacturer, a quality assurance manager,

a technologist, and a radiologist, must perform when implementing the profile.

The American Institute of Ultrasound in Medicine (AIUM) formed the Liver Fat Quantification Task Force in 2019, comprised of academic physicians, physicists and engineers, and representatives from US manufacturers, pharmaceutical companies, and government agencies. The Task Force goals are to (a) advocate for liver fat quantification techniques; (b) advise on the development of new techniques, such as preferred reference standards and target diagnostic performance; and (c) provide recommendations during the translation of emerging techniques into clinical practice, including use cases and target populations, acquisition techniques, and reporting. It was clear that knowledge regarding the diagnostic performance of the many possible emerging techniques, and inter- and intra-manufacturer variability, was needed to achieve these goals. Members of the AIUM Liver Fat Quantification Task Force and AIUM leadership joined ongoing efforts within the RSNA QIBA regarding the formation of a new biomarker committee to address the need for the technical standardization of AC, BC, and SOS measures.

The AIUM–RSNA QIBA Pulse-Echo Quantitative Ultrasound Biomarker Committee was created in 2020 to address the interests of the AIUM Liver Fat Quantification Task Force and to reach consensus on how to measure, report, and test PEQUS features, among manufacturers and under equivalent conditions, to be used as biomarkers for hepatic steatosis.

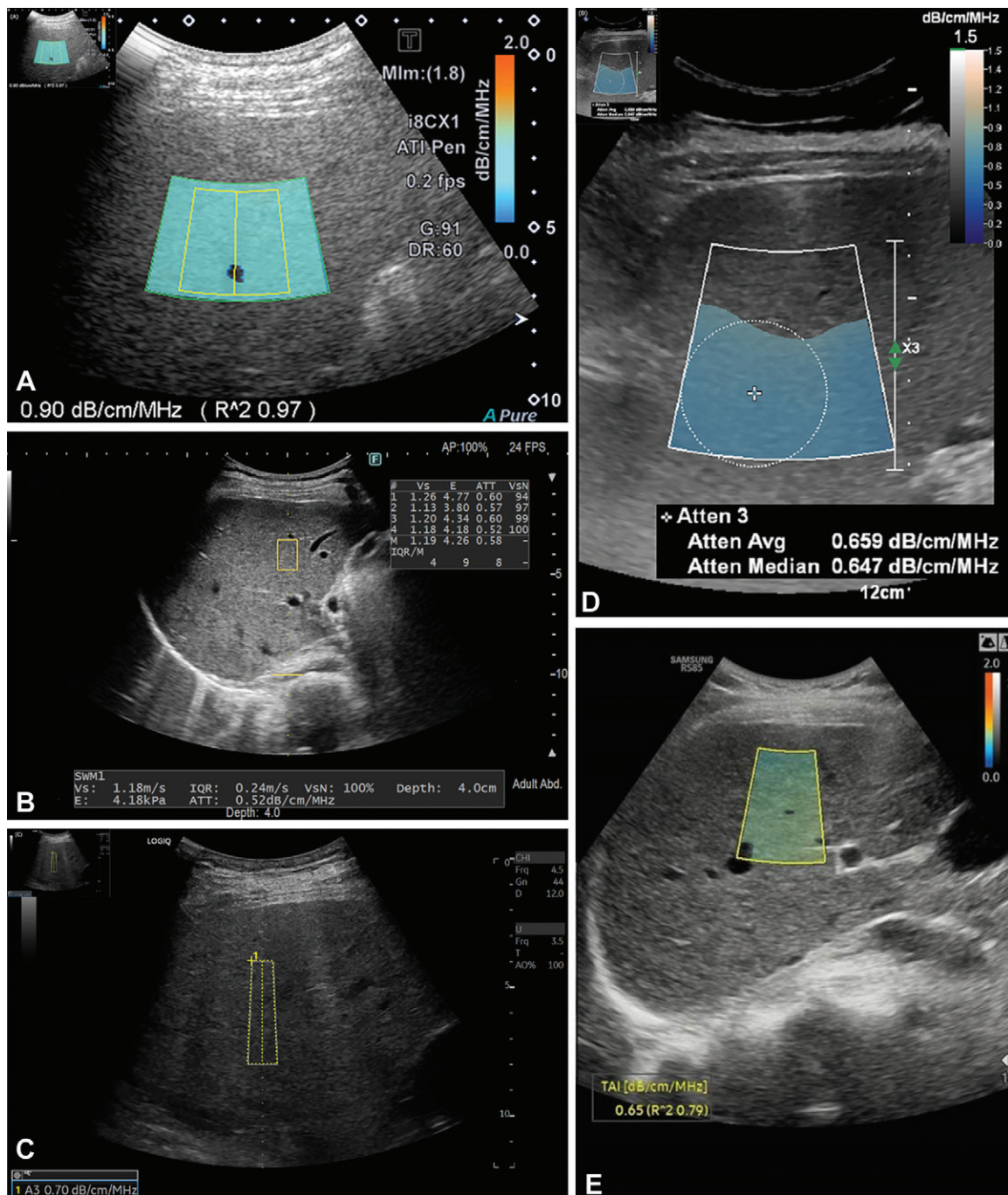


Figure 3: US images show various commercial implementations of the attenuation coefficient, including (A) ATI (Canon Medical Systems), (B) ATT (FujiFilm Medical Systems), (C) UGAP (GE Healthcare), (D) Atten (Philips Healthcare), and (E) TAI (Samsung Medison). Images A, C, and D were acquired at the Massachusetts General Hospital Center for Ultrasound Research & Translation laboratory as a component of the Non-Invasive Biomarkers of Metabolic Liver Disease (NIMBLE) study, which is supported by the Foundation for the National Institutes of Health and the private sector.

To address the challenge of assessing the technical and clinical performance of multiple possible biomarkers, a three-level framework was defined by the biomarker committee as follows: (a) single biomarker measurement level, focused on establishing measurement standards to reduce variability and bias when measuring a given physical parameter (eg, measuring attenuation in a manner that minimizes variability and bias); (b) single biomarker predictor level, developed jointly with the AIUM Liver Fat Quantification Task Force and aimed at demonstrating

the relationship between the individual biomarker and the biologic concept of interest (eg, demonstrating the relationship between hepatic steatosis and attenuation, measured in the manner recommended at the single biomarker measurement level); and (c) multiple biomarker predictor level, focused on investigating the relationship between multiple simultaneous biomarker measurements and the biologic concept of interest (eg, developing a model that combines AC, BC, and SOS to create a synthetic biomarker for liver steatosis).

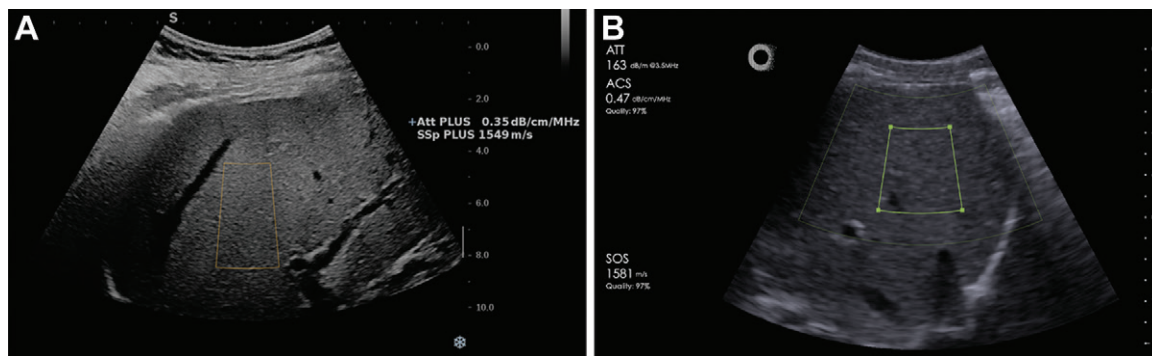


Figure 4: US images show commercial implementations of the attenuation coefficient and speed of sound, including (A) Att and SSp (Hologic Supersonic Imagine) and (B) ACS and SOS (E-Scopics).



Figure 5: US image shows sound speed index (SSI) quantification by Mindray, a commercial implementation of the speed of sound.

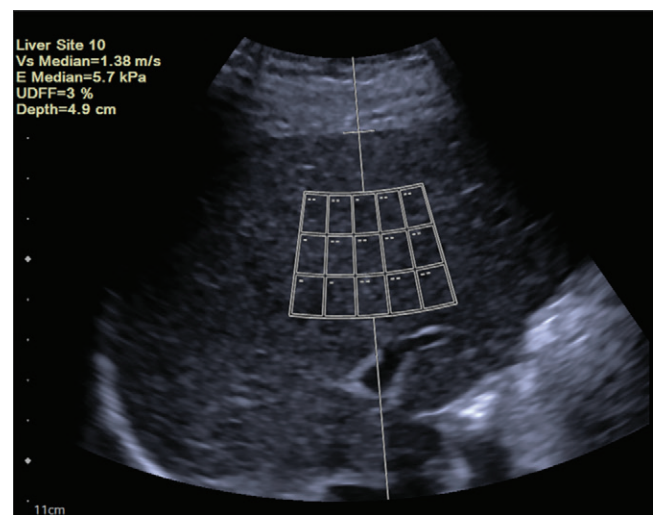


Figure 6: US image shows a fat fraction tool (Siemens Healthineers) derived from pulse-echo quantitative US features. The image was acquired at the Massachusetts General Hospital Center for Ultrasound Research & Translation laboratory as a component of the Non-Invasive Biomarkers of Metabolic Liver Disease (NIMBLE) study, which is supported by the Foundation for the National Institutes of Health and the private sector.

The single biomarker measurement level is the current focus of the PEQUS biomarker committee. Current activities are based on developing the biomarker profile and releasing it for public comment.

AIUM–RSNA QIBA PEQUS Committee Groundwork

Standardization of measurement results across devices from different manufacturers is important. Inconsistent measurement values among devices have multiple negative consequences, including confusion for interpreting physicians (the end users), misdiagnosis, and requirement for duplicate studies with different systems, which may increase costs. All these factors can hamper clinical adoption of a new feature or technology, even when that technology shows great promise. To help standardize PEQUS biomarker measurements, the AIUM–RSNA QIBA PEQUS biomarker committee is planning a prospective, multisite liver-mimicking phantom study, with the goal of defining lower bounds of bias, repeatability, and reproducibility in phantoms with ranges of acoustic properties (AC, BC, SOS) that are relevant to the disease of interest (ie, NAFLD).

One challenge of this study is creating a method to specify the phantom properties. The SOS and AC are relatively straightforward to characterize and control in a phantom

(96–98). SOS has very little frequency dependence in the range of frequencies used for diagnostic US. Attenuation is approximately proportional to frequency and is specified in units of decibels per centimeter of megahertz (dB/cm-MHz). BC is dependent on frequency and is typically controlled through the inclusion of microscopic glass or ceramic beads, graphite powder, or other fine particles. To emulate a variety of tissue types, a range of scatterer sizes that provides levels of scattering similar to those observed in healthy and steatotic liver is proposed for the phantoms in the study. Considering these challenges, we have specified four phantoms with acoustic properties within the ranges expected for steatotic liver ($0.5 \leq AC \leq 1.0$ dB/cm-MHz, $4 \times 10^{-4} \leq BC \leq 10^{-1}$ 1/cm-Sr at 3MHz, and $1500 \leq SOS \leq 1580$ m/sec). In addition, because methods for analyzing the BC typically require a reference phantom with a known AC and BC, this study will include two additional phantoms with known properties for use in reference phantom studies. Reference AC, BC, and SOS values of the phantoms will be measured using

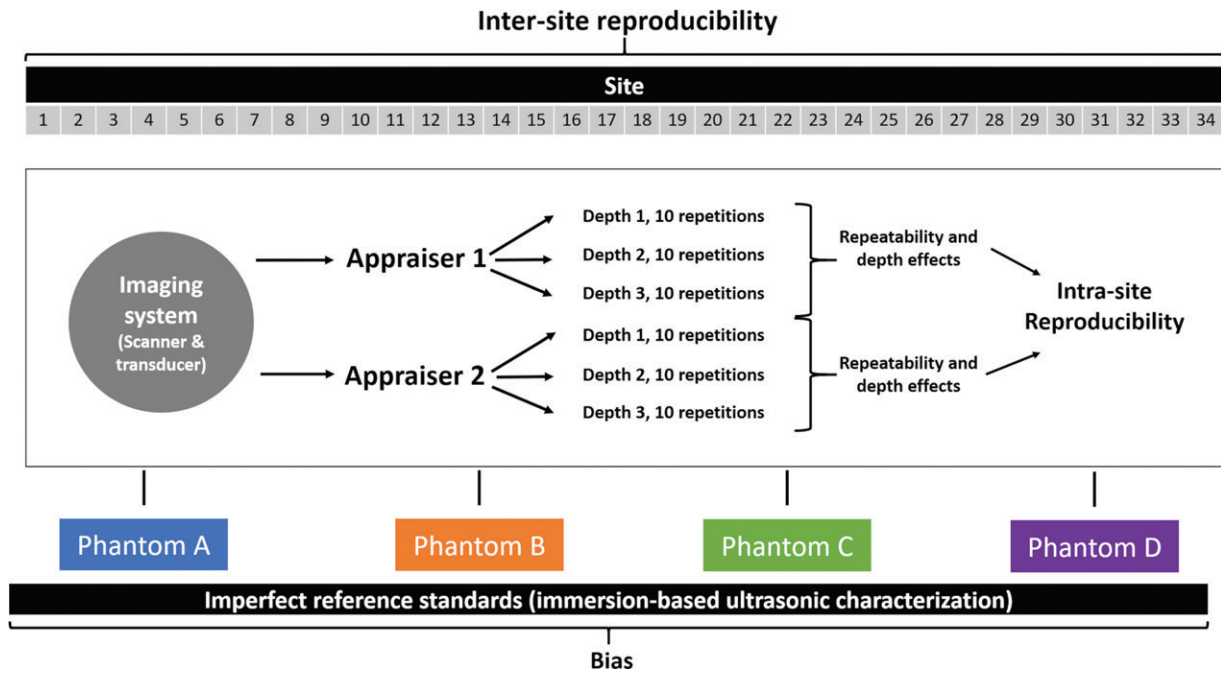


Figure 7: Diagram depicts the strategy for the phantom-based groundwork study planned by the American Institute of Ultrasound in Medicine–RSNA Quantitative Imaging Biomarkers Alliance Pulse-Echo Quantitative Ultrasound Biomarker Committee. The study will include the participation of 10 US vendors and 24 clinical, academic, and government institutions for an expected total of 34 sites. At least three sites will perform measurements on at least one specified imaging system from each vendor. Each site will perform measurements on the four phantoms with two appraisers, and each appraiser will perform 10 repetitions at three different depths.

well-accepted immersion-based techniques with single-element piezoelectric transducers (99,100). These values will be used in the analysis of bias.

The planned study will include the participation of 10 US vendors who have implemented PEQUS features on their systems, as well as 24 clinical, academic, and government institutions from North and South America, Europe, and Asia. Each vendor will specify the imaging system (scanner model, transducer, and software version) to be tested in the study. At least three sites will perform measurements on at least one specified imaging system from each vendor. Each site will perform measurements on the four phantoms with two appraisers, and each appraiser will perform 10 repetitions at three different depths (Fig 7). This strategy will allow us to assess intraoperator and interoperator variability, as well as intersite and intervendor reproducibility. Statistical analysis will follow the strategy defined by the QIBA technical performance working group (95). In addition, each biomarker working group within the PEQUS biomarker committee will define specific questions to address during the study, which will depend on the extent of evidence on technical performance available in the literature. These questions include, for example, whether the values of the biomarkers vary with the depth or estimation algorithm. It is important to note that only PEQUS techniques supported by evidence of continuous development in the literature (simulations, phantom-based studies, preclinical and clinical implementations) will be included in the study. The results from the study will be used to refine the draft of claims included in the first versions of the PEQUS biomarker committee profiles.

Challenges and Perspectives

The goals of the AIUM Liver Fat Quantification Task Force and AIUM–RSNA QIBA PEQUS biomarker committee require convergence of the interests of multiple stakeholders, including clinicians, academics, government experts, and industry partners. These interests are considered within the scientific activities of QIBA, such as the proposed multisite phantom study, which will help define the diagnostic performance of PEQUS methods. A better understanding of the sources of measurement bias and variability will ultimately help manufacturers to minimize them across systems and to realize the benefits of PEQUS quantitative imaging biomarkers for liver fat quantification.

The biggest challenge facing US manufacturers is meeting the cost of compliance to agreed-upon standards. For vendors that already have a commercial implementation of a technology, there is a high cost to make changes. This is especially so when there is an established user base and experience. With the large number of US vendors engaged in liver fat quantification methods, there is substantial opportunity for divergence in methods and, consequently, a large effort may be needed to harmonize methods that have evolved independently. However, there is an even greater cost to patient care and the industry as a whole if measurements are not repeatable and comparable across devices.

Besides the value of measurement, additional features of fat quantification tools on US systems could influence outcomes (quality metrics), visualization tools (color maps), and reporting metrics (fat percentage or steatosis stage). Standardization of these features across systems will also reduce user confusion and, hopefully, improve adoption. Continuous feedback between manufacturers and end users will help refine the measurement

protocol, technique, and interpretation. The AIUM and QIBA initiatives provide manufacturers with an opportunity to work with clinical, academic, and government experts to reach consensus on many of these challenges. Guidance from organizations such as AIUM and QIBA is valuable for designing the appropriate user interface and the necessary tools that will enable users to perform quantitative imaging biomarker measurement efficiently and consistently.

Conclusion

The pathophysiologic complexity of liver disease creates challenges in the validation of practical quantitative imaging biomarkers such as those for liver steatosis. Imaging biomarkers based on diagnostic US hold great potential due to the widespread availability, safety, and relatively low cost of US systems, and these factors will likely impact adoption of such biomarkers for screening, surveillance, and patient management. The recent introduction by US system manufacturers of pulse-echo quantitative US imaging measures, including the attenuation coefficient, backscatter coefficient, and speed of sound, represents significant progress in this direction. However, coordinated efforts among end users, manufacturers, academics, and government and clinical experts to standardize the implementation of these new technologies will be essential to achieve their full potential as biomarkers.

Acknowledgments: We thank all the members of the AIUM Liver Fat Quantification Task Force, the members of the AIUM-RSNA QIBA Pulse-Echo Quantitative Ultrasound Biomarker Committee (complete roster at https://qibawiki.rsna.org/index.php/AIUM/QIBA_Pulse-Echo_Quantitative_Ultrasound_Biomarker_Cite), and our industry partners for the valuable discussions reflected in the content of this review. We also thank Theodore Pierce, MD, for his help in collecting example images from commercial implementations of PEQUUS features.

Disclosures of conflicts of interest: **D.T.F.** Institutional research agreements with and material support from GE Healthcare, Philips Healthcare, and Siemens Healthineers; advisory board consulting fees from GE Healthcare and Philips Healthcare. **I.M.R.M.** Research agreements with and equipment loans from Siemens Healthineers and General Electric; consultant, Siemens Healthineers; patents planned, issued, or pending; co-chair, American Institute of Ultrasound in Medicine (AIUM)-RSNA Quantitative Imaging Biomarkers Alliance (QIBA) Pulse-Echo Quantitative Ultrasound (PEQUUS) Committee; member, Imaging Metrology and Standards Subcommittee and Ultrasound Subcommittee of the American Association of Physicists in Medicine. **M.W.** Meeting attendance support from GE Healthcare; co-chair, RSNA QIBA PEQUUS Committee. **M.L.R.** New ultrasound equipment evaluation and lecture payment, Philips Medical; lecture payment, World Federation of Ultrasound in Medicine and Biology; associate editor, *Radiology*; subspecialty editor, *Journal of Ultrasound in Medicine*; editorial board, *Ultrasound Quarterly*. **A.O.** No relevant relationships. **K.A.W.** Royalties from CIRS; patents planned, issued, or pending; research agreement with Siemens Healthineers; chair, AIUM Bioeffects Committee and AAPM Task Group 333 MR-guided Focused Ultrasound Quality Assurance; member, AAPM TG353-Pulsed Doppler and Color Flow Ultrasound System Performance Assessment using Flow Phantoms, AIUM Technical Standards Committee, AIUM QIBA PEQUUS Biomarker Committee, AIUM QIBA Shear Wave Speed Biomarker Committee, and AIUM QIBA Coordinating Committee; editorial board, *The Journal of the Acoustical Society of America* and *Ultrasonic Imaging*. **J.O.** No relevant relationships. **T.A.S.** Internal startup funding and participation on a data safety monitoring board, Kettering University; consultant, Riverside Research. **J.B.F.** Board member and meeting attendance support, AIUM and International Contrast Ultrasound Society; grant or equipment support from Philips Healthcare and GE Healthcare. **T.J.H.** Grants or contracts from Siemens Healthineers, General Electric, Philips, Samsung, Clarius, Echoscens, and Mindray; chair, RSNA QIBA; equipment loans and technical support, Siemens Healthineers. **A.E.S.** Institutional payments, Allergan, Analogic Corporation, Boehringer Ingelheim, Department of Defense, Echoscens, Fujifilm Healthcare, Foundation for the National Institutes of Health (NIH), Genentech, General Electric, Gilead, Intercept, Medimmune, NIH, Novo Nordisk, Partners Healthcare, Philips, Supersonic Imagine, Takeda, Toshiba

Medical Systems, and Siemens; royalties or licenses, Elsevier and Katharos Labs; consulting fees, Astra Zeneca, Bracco Diagnostics, Bristol-Myers Squibb, General Electric, Gerson Lehman Group, Guidepoint Global Advisors, Supersonic Imagine, Novartis, Pfizer, Philips, Parexel Informatics, and WorldCare Clinical; legal consulting, Matis Baum and O'Connor; board of governors, AIUM; stockholder, Oehre Bio, Rhino Healthtech, Katharos Labs, Avira, Autonomous, Quantix Bio, Evidence Based Psychology, and Klea.

References

1. Younossi ZM, Koenig AB, Abdelatif D, Fazel Y, Henry L, Wymer M. Global epidemiology of nonalcoholic fatty liver disease—Meta-analytic assessment of prevalence, incidence, and outcomes. *Hepatology* 2016;64(1):73–84.
2. Eslam M, Sanyal AJ, George J; International Consensus Panel. MAFLD: A consensus-driven proposed nomenclature for metabolic associated fatty liver disease. *Gastroenterology* 2020;158(7):1999–2014.e1.
3. Chalasani N, Younossi Z, Lavine JE, et al. The diagnosis and management of nonalcoholic fatty liver disease: Practice guidance from the American Association for the Study of Liver Diseases. *Hepatology* 2018;67(1):328–357.
4. Hamer OW, Aguirre DA, Casola G, Lavine JE, Woenckhaus M, Sirlin CB. Fatty liver: imaging patterns and pitfalls. *RadioGraphics* 2006;26(6):1637–1653.
5. Brunt EM, Janney CG, DiBisceglie AM, Neuschwander-Tetri BA, Bacon BR. Nonalcoholic steatohepatitis: a proposal for grading and staging the histological lesions. *Am J Gastroenterol* 1999;94(9):2467–2474.
6. Loomba R, Sanyal AJ. The global NAFLD epidemic. *Nat Rev Gastroenterol Hepatol* 2013;10(11):686–690.
7. Goldberg D, Ditah IC, Saedian K, et al. Changes in the prevalence of hepatitis C virus infection, nonalcoholic steatohepatitis, and alcoholic liver disease among patients with cirrhosis or liver failure on the waitlist for liver transplantation. *Gastroenterology* 2017;152(5):1090–1099.e1.
8. European Association for the Study of the Liver (EASL); European Association for the Study of Diabetes (EASD); European Association for the Study of Obesity (EASO). EASL-EASD-EASO Clinical Practice Guidelines for the management of non-alcoholic fatty liver disease. *J Hepatol* 2016;64(6):1388–1402.
9. Kim SR, Lerman LO. Diagnostic imaging in the management of patients with metabolic syndrome. *Transl Res* 2018;194(1):1–18.
10. Ajmera V, Park CC, Caussy C, et al. Magnetic resonance imaging proton density fat fraction associates with progression of fibrosis in patients with nonalcoholic fatty liver disease. *Gastroenterology* 2018;155(2):307–310.e2.
11. Noureddin M, Lam J, Peterson MR, et al. Utility of magnetic resonance imaging versus histology for quantifying changes in liver fat in nonalcoholic fatty liver disease trials. *Hepatology* 2013;58(6):1930–1940.
12. Caussy C, Reeder SB, Sirlin CB, Loomba R. Noninvasive, quantitative assessment of liver fat by MRI-PDFF as an endpoint in NASH trials. *Hepatology* 2018;68(2):763–772.
13. Patel J, Bettencourt R, Cui J, et al. Association of noninvasive quantitative decline in liver fat content on MRI with histologic response in nonalcoholic steatohepatitis. *Therap Adv Gastroenterol* 2016;9(5):692–701.
14. Geier A, Tiniakos D, Denk H, Trauner M. From the origin of NASH to the future of metabolic fatty liver disease. *Gut* 2021;70(8):1570–1579.
15. Khalifa A, Rockey DC. The utility of liver biopsy in 2020. *Curr Opin Gastroenterol* 2020;36(3):184–191.
16. Kleiner DE, Brunt EM, Van Natta M, et al. Design and validation of a histological scoring system for nonalcoholic fatty liver disease. *Hepatology* 2005;41(6):1313–1321.
17. Goldstein NS, Hastah F, Galan MV, Gordon SC. Fibrosis heterogeneity in nonalcoholic steatohepatitis and hepatitis C virus needle core biopsy specimens. *Am J Clin Pathol* 2005;123(3):382–387.
18. Ratziu V, Charlotte F, Heurtier A, et al. Sampling variability of liver biopsy in nonalcoholic fatty liver disease. *Gastroenterology* 2005;128(7):1898–1906.
19. Regev A, Berho M, Jeffers LJ, et al. Sampling error and intraobserver variation in liver biopsy in patients with chronic HCV infection. *Am J Gastroenterol* 2002;97(10):2614–2618.
20. Expert Panel on Gastrointestinal Imaging; Bashir MR, Horowitz JM, et al. ACR Appropriateness Criteria® Chronic Liver Disease. *J Am Coll Radiol* 2020;17(5S):S70–S80.
21. Rockey DC, Caldwell SH, Goodman ZD, Nelson RC, Smith AD; American Association for the Study of Liver Diseases. Liver biopsy. *Hepatology* 2009;49(3):1017–1044.
22. FDA-NIH Biomarker Working Group. BEST (Biomarkers, EndpointS, and other Tools) Resource. Silver Spring (MD): Food and Drug Administration (US). <https://www.ncbi.nlm.nih.gov/books/NBK326791/>. Published 2016. Accessed June 1, 2021.

23. Zhou JH, Cai JJ, She ZG, Li HL. Noninvasive evaluation of nonalcoholic fatty liver disease: Current evidence and practice. *World J Gastroenterol* 2019;25(11):1307–1326.
24. Vilar-Gomez E, Chalasani N. Non-invasive assessment of non-alcoholic fatty liver disease: Clinical prediction rules and blood-based biomarkers. *J Hepatol* 2018;68(2):305–315.
25. Petroff D, Blank V, Newsome PN, et al. Assessment of hepatic steatosis by controlled attenuation parameter using the M and XL probes: an individual patient data meta-analysis. *Lancet Gastroenterol Hepatol* 2021;6(3):185–198.
26. Newsome PN, Sasso M, Deeks JJ, et al. FibroScan-AST (FAST) score for the non-invasive identification of patients with non-alcoholic steatohepatitis with significant activity and fibrosis: a prospective derivation and global validation study. *Lancet Gastroenterol Hepatol* 2020;5(4):362–373.
27. Karlas T, Petroff D, Sasso M, et al. Individual patient data meta-analysis of controlled attenuation parameter (CAP) technology for assessing steatosis. *J Hepatol* 2017;66(5):1022–1030.
28. Vuppalanchi R, Siddiqui MS, Van Natta ML, et al. Performance characteristics of vibration-controlled transient elastography for evaluation of nonalcoholic fatty liver disease. *Hepatology* 2018;67(1):134–144.
29. Zhang X, Wong GLH, Wong VWS. Application of transient elastography in nonalcoholic fatty liver disease. *Clin Mol Hepatol* 2020;26(2):128–141.
30. Yajima Y, Narui T, Ishii M, et al. Computed tomography in the diagnosis of fatty liver: total lipid content and computed tomography number. *Tohoku J Exp Med* 1982;136(3):337–342.
31. Ma X, Holalkere NS, Kambadakone R A, Mino-Kenudson M, Hahn PF, Sahani DV. Imaging-based quantification of hepatic fat: methods and clinical applications. *RadioGraphics* 2009;29(5):1253–1277.
32. Starekova J, Hernandez D, Pickhardt PJ, Reeder SB. Quantification of liver fat content with CT and MRI: state of the art. *Radiology* 2021;301(2):250–262.
33. Fischer MA, Gnannt R, Raptis D, et al. Quantification of liver fat in the presence of iron and iodine: an ex-vivo dual-energy CT study. *Invest Radiol* 2011;46(6):351–358.
34. Ma J, Song ZQ, Yan FH. Separation of hepatic iron and fat by dual-source dual-energy computed tomography based on material decomposition: an animal study. *PLoS One* 2014;9(10):e110964.
35. Artz NS, Hines CDG, Brunner ST, et al. Quantification of hepatic steatosis with dual-energy computed tomography: comparison with tissue reference standards and quantitative magnetic resonance imaging in the ob/ob mouse. *Invest Radiol* 2012;47(10):603–610.
36. Li Q, Dhyani M, Grajo JR, Sirlin C, Samir AE. Current status of imaging in nonalcoholic fatty liver disease. *World J Hepatol* 2018;10(8):530–542.
37. Pickhardt PJ, Graffy PM, Perez AA, Lubner MG, Elton DC, Summers RM. Opportunistic screening at abdominal CT: use of automated body composition biomarkers for added cardiometabolic value. *RadioGraphics* 2021;41(2):524–542.
38. Yokoo T, Serai SD, Pirasteh A, et al. Linearity, bias, and precision of hepatic proton density fat fraction measurements by using MR imaging: A meta-analysis. *Radiology* 2018;286(2):486–498.
39. Tang A, Tan J, Sun M, et al. Nonalcoholic fatty liver disease: MR imaging of liver proton density fat fraction to assess hepatic steatosis. *Radiology* 2013;267(2):422–431.
40. Idilman IS, Keskin O, Celik A, et al. A comparison of liver fat content as determined by magnetic resonance imaging-proton density fat fraction and MRS versus liver histology in non-alcoholic fatty liver disease. *Acta Radiol* 2016;57(3):271–278.
41. Tang A, Desai A, Hamilton G, et al. Accuracy of MR imaging-estimated proton density fat fraction for classification of dichotomized histologic steatosis grades in nonalcoholic fatty liver disease. *Radiology* 2015;274(2):416–425.
42. Hernaez R, Lazo M, Bonekamp S, et al. Diagnostic accuracy and reliability of ultrasonography for the detection of fatty liver: a meta-analysis. *Hepatology* 2011;54(3):1082–1090.
43. Paige JS, Bernstein GS, Heba E, et al. A pilot comparative study of quantitative ultrasound, conventional ultrasound, and MRI for predicting histology-determined steatosis grade in adult nonalcoholic fatty liver disease. *AJR Am J Roentgenol* 2017;208(5):W168–W177.
44. Strauss S, Gavish E, Gottlieb P, Katsnelson L. Interobserver and intraobserver variability in the sonographic assessment of fatty liver. *AJR Am J Roentgenol* 2007;189(6):W320–W323.
45. Marshall RH, Eissa M, Bluth EI, Gulotta PM, Davis NK. Hepatorenal index as an accurate, simple, and effective tool in screening for steatosis. *AJR Am J Roentgenol* 2012;199(5):997–1002.
46. Pirmoazen AM, Khurana A, Loening AM, et al. Diagnostic performance of 9 quantitative ultrasound parameters for detection and classification of hepatic steatosis in nonalcoholic fatty liver disease. *Invest Radiol* 2022;57(1):23–32.
47. Chauhan A, Sultan LR, Furth EE, Jones LP, Khungar V, Sehgal CM. Diagnostic accuracy of hepatorenal index in the detection and grading of hepatic steatosis. *J Clin Ultrasound* 2016;44(9):580–586.
48. Ferraioli G, Monteiro LB. Ultrasound-based techniques for the diagnosis of liver steatosis. *World J Gastroenterol* 2019;25(40):6053–6062.
49. Bigelow TA, Labyed Y. Attenuation compensation and estimation. In: Mamou J, Oelze ML, eds. *Quantitative ultrasound in soft tissues*. Dordrecht, the Netherlands: Springer, 2013; 71–93.
50. Garra BS, Insana MF, Shawker TH, Russell MA. Quantitative estimation of liver attenuation and echogenicity: normal state versus diffuse liver disease. *Radiology* 1987;162(1 Pt 1):61–67.
51. Itoh K, Yasuda Y, Suzuki O, et al. Studies on frequency-dependent attenuation in the normal liver and spleen and in liver diseases, using the spectral-shift zero-crossing method. *J Clin Ultrasound* 1988;16(8):553–562.
52. Kuni CC, Johnson TK, Crass JR, Snover DC. Correlation of Fourier spectral shift-determined hepatic acoustic attenuation coefficients with liver biopsy findings. *J Ultrasound Med* 1989;8(11):631–634.
53. Taylor KJ, Riely CA, Hammers L, et al. Quantitative US attenuation in normal liver and in patients with diffuse liver disease: importance of fat. *Radiology* 1986;160(1):65–71.
54. Ferraioli G, Maiocchi L, Savietto G, et al. Performance of the attenuation imaging technology in the detection of liver steatosis. *J Ultrasound Med* 2021;40(7):1325–1332.
55. Jang JK, Choi SH, Lee JS, Kim SY, Lee SS, Kim KW. Accuracy of the ultrasound attenuation coefficient for the evaluation of hepatic steatosis: a systematic review and meta-analysis of prospective studies. *Ultrasonography* 2022;41(1):83–92.
56. Labyed Y, Bigelow TA. A theoretical comparison of attenuation measurement techniques from backscattered ultrasound echoes. *J Acoust Soc Am* 2011;129(4):2316–2324.
57. Pirmoazen AM, Khurana A, El Kaffas A, Kamaya A. Quantitative ultrasound approaches for diagnosis and monitoring hepatic steatosis in nonalcoholic fatty liver disease. *Theranostics* 2020;10(9):4277–4289.
58. Insana MF, Brown DG. Acoustic scattering theory applied to soft biological tissues. In: Shung KK, Thieme GA, eds. *Ultrasonic scattering in biological tissues*. Boca Raton, Fla: CRC Press, 1993.
59. Yao LX, Zagzebski JA, Madsen EL. Backscatter coefficient measurements using a reference phantom to extract depth-dependent instrumentation factors. *Ultrasound Imaging* 1990;12(1):58–70.
60. Guerrero QW, Fan L, Brunke S, Milkowski A, Rosado-Mendez IM, Hall TJ. Power spectrum consistency among systems and transducers. *Ultrasound Med Biol* 2018;44(11):2358–2370.
61. Labyed Y, Milkowski A. Novel method for ultrasound-derived fat fraction using an integrated phantom. *J Ultrasound Med* 2020;39(12):2427–2438.
62. O'Donnell M, Miller JG. Quantitative broadband ultrasonic backscatter: An approach to nondestructive evaluation in acoustically inhomogeneous materials. *J Appl Phys* 1981;52(2):1056–1065.
63. Wear KA, Garra BS, Hall TJ. Measurements of ultrasonic backscatter coefficients in human liver and kidney in vivo. *J Acoust Soc Am* 1995;98(4):1852–1857.
64. Lin SC, Heba E, Wolfson T, et al. Noninvasive diagnosis of nonalcoholic fatty liver disease and quantification of liver fat using a new quantitative ultrasound technique. *Clin Gastroenterol Hepatol* 2015;13(7):1337–1345.e6.
65. Han A, Zhang YN, Boehringer AS, et al. Assessment of hepatic steatosis in nonalcoholic fatty liver disease by using quantitative US. *Radiology* 2020;295(1):106–113.
66. Lu ZF, Zagzebski JA, Lee FT. Ultrasound backscatter and attenuation in human liver with diffuse disease. *Ultrasound Med Biol* 1999;25(7):1047–1054.
67. Oelze ML, O'Brien WJ Jr. Frequency-dependent attenuation-compensation functions for ultrasonic signals backscattered from random media. *J Acoust Soc Am* 2002;111(5 Pt 1):2308–2319.
68. Samir AE, Dhyani M, Vij A, et al. Shear-wave elastography for the estimation of liver fibrosis in chronic liver disease: determining accuracy and ideal site for measurement. *Radiology* 2015;274(3):888–896.
69. Ferraioli G, Wong VWS, Castera L, et al. Liver Ultrasound Elastography: An Update to the World Federation for Ultrasound in Medicine and Biology Guidelines and Recommendations. *Ultrasound Med Biol* 2018;44(12):2419–2440.
70. Han A, Andre MP, Deiranieh L, et al. Repeatability and reproducibility of the ultrasonic attenuation coefficient and backscatter coefficient measured

- in the right lobe of the liver in adults with known or suspected nonalcoholic fatty liver disease. *J Ultrasound Med* 2018;37(8):1913–1927.
71. Barr RG, Ferraioli G, Palmeri ML, et al. Elastography assessment of liver fibrosis: Society of Radiologists in Ultrasound consensus conference statement. *Radiology* 2015;276(3):845–861.
 72. Sarvazyan AP, Urban MW, Greenleaf JF. Acoustic waves in medical imaging and diagnostics. *Ultrasound Med Biol* 2013;39(7):1133–1146.
 73. Barr RG. Shear wave liver elastography. *Abdom Radiol (NY)* 2018;43(4):800–807.
 74. Hayashi N, Tamaki N, Senda M, et al. A new method of measuring in vivo sound speed in the reflection mode. *J Clin Ultrasound* 1988;16(2):87–93.
 75. Napolitano D, Chou CH, McLaughlin G, et al. Sound speed correction in ultrasound imaging. *Ultrasonics* 2006;44(Suppl 1):e43–e46.
 76. Dioguardi Burgio M, Ronot M, Reizine E, et al. Quantification of hepatic steatosis with ultrasound: promising role of attenuation imaging coefficient in a biopsy-proven cohort. *Eur Radiol* 2020;30(4):2293–2301.
 77. Bendjador H, Deffieux T, Tanter M. SVD beamforming for ultrafast aberration correction and real-time speed-of-sound quantification. In: 2020 IEEE International Ultrasonics Symposium (IUS), Las Vegas, NV, September 7–11, 2020. Piscataway, NJ: IEEE, 2020; 1–4. <https://doi.org/10.1109/IUS46767.2020.9251435>.
 78. Imbault M, Dioguardi Burgio M, Faccinnetto A, et al. Ultrasonic fat fraction quantification using in vivo adaptive sound speed estimation. *Phys Med Biol* 2018;63(21):215013.
 79. Jaeger M, Robinson E, Akarçay HG, Frenz M. Full correction for spatially distributed speed-of-sound in echo ultrasound based on measuring aberration delays via transmit beam steering. *Phys Med Biol* 2015;60(11):4497–4515.
 80. Stähli P, Kuriakose M, Frenz M, Jaeger M. Improved forward model for quantitative pulse-echo speed-of-sound imaging. *Ultrasonics* 2020;108:106168.
 81. Stähli P, Frenz M, Jaeger M. Bayesian approach for a robust speed-of-sound reconstruction using pulse-echo ultrasound. *IEEE Trans Med Imaging* 2021;40(2):457–467.
 82. Lin T, Ophir J, Potter G. Correlations of sound speed with tissue constituents in normal and diffuse liver disease. *Ultrason Imaging* 1987;9(1):29–40.
 83. Zubajlo RE, Benjamin A, Grajo JR, et al. Experimental validation of longitudinal speed of sound estimates in the diagnosis of hepatic steatosis (part II). *Ultrasound Med Biol* 2018;44(12):2749–2758.
 84. Chen CF, Robinson DE, Wilson LS, Griffiths KA, Manoharan A, Doust BD. Clinical sound speed measurement in liver and spleen in vivo. *Ultrason Imaging* 1987;9(4):221–235.
 85. Robinson DE, Chen F, Wilson LS. Measurement of velocity of propagation from ultrasonic pulse-echo data. *Ultrasound Med Biol* 1982;8(4):413–420.
 86. Bamber JC, Hill CR. Acoustic properties of normal and cancerous human liver-I. Dependence on pathological condition. *Ultrasound Med Biol* 1981;7(2):121–133.
 87. Boozari B, Pothoff A, Mederacke I, et al. Evaluation of sound speed for detection of liver fibrosis: prospective comparison with transient dynamic elastography and histology. *J Ultrasound Med* 2010;29(11):1581–1588.
 88. Popa A, Şirli R, Popescu A, et al. Ultrasound-based quantification of fibrosis and steatosis with a new software considering transient elastography as reference in patients with chronic liver diseases. *Ultrasound Med Biol* 2021;47(7):1692–1703.
 89. Dioguardi Burgio M, Imbault M, Ronot M, et al. Ultrasonic adaptive sound speed estimation for the diagnosis and quantification of hepatic steatosis: a pilot study. *Ultraschall Med* 2019;40(6):722–733.
 90. Imbault M, Faccinnetto A, Osmanski BF, et al. Robust sound speed estimation for ultrasound-based hepatic steatosis assessment. *Phys Med Biol* 2017;62(9):3582–3598.
 91. Kumagai H, Taniguchi N, Yokoyama K, et al. The speed of sound in rat liver with steatohepatitis: ex vivo analysis using two types of ultrasound systems. *Ultrasound Med Biol* 2019;45(8):2258–2265.
 92. Ormachea J, Parker KJ. A Preliminary Study of Liver Fat Quantification Using Reported Ultrasound Speed of Sound and Attenuation Parameters. *Ultrasound Med Biol* 2022;48(4):675–684.
 93. Kessler LG, Barnhart HX, Buckler AJ, et al. The emerging science of quantitative imaging biomarkers terminology and definitions for scientific studies and regulatory submissions. *Stat Methods Med Res* 2015;24(1):9–26.
 94. Sullivan DC, Obuchowski NA, Kessler LG, et al. Metrology Standards for Quantitative Imaging Biomarkers. *Radiology* 2015;277(3):813–825.
 95. Raunig DL, McShane LM, Pennello G, et al. Quantitative imaging biomarkers: a review of statistical methods for technical performance assessment. *Stat Methods Med Res* 2015;24(1):27–67.
 96. Madsen EL, Zagzebski JA, Banjavie RA, Jutila RE. Tissue mimicking materials for ultrasound phantoms. *Med Phys* 1978;5(5):391–394.
 97. Madsen EL, Zagzebski JA, Frank GR. Oil-in-gelatin dispersions for use as ultrasonically tissue-mimicking materials. *Ultrasound Med Biol* 1982;8(3):277–287.
 98. Madsen EL, Zagzebski JA, Insana MF, Burke TM, Frank G. Ultrasonically tissue-mimicking liver including the frequency dependence of backscatter. *Med Phys* 1982;9(5):703–710.
 99. Madsen EL, Dong F, Frank GR, et al. Interlaboratory comparison of ultrasonic backscatter, attenuation, and speed measurements. *J Ultrasound Med* 1999;18(9):615–631.
 100. Chen JF, Zagzebski JA, Madsen EL. Tests of backscatter coefficient measurement using broadband pulses. *IEEE Trans Ultrason Ferroelectr Freq Control* 1993;40(5):603–607.